Development of Low-Irreversibility Engines

Investigators

C.F. Edwards, Associate Professor, Mechanical Engineering; K.-Y. Teh, S.L. Miller, Graduate Researchers.

Introduction

An *engine* is a device that converts some fraction of the energy in a resource into work. The most work that can be developed by a particular engine design is its *reversible* work. The *irreversibility* of an engine is the difference between the reversible work that it could develop and the actual work that it performs; it is the lost work. In this research we investigate the potential to design and implement engines with significantly reduced irreversibility, and thereby, improved efficiency.

The relevance of this work to the objective of GCEP is that significant improvements in efficiency are one of the most effective approaches to reducing greenhouse-gas emissions. Since the approach we take is fundamental and comprehensive, it enables improvements with fuels (such as existing hydrocarbons and possible future hydrogen fuel), and with engines (such as those for transportation, propulsion, and electrical power generation).

Background

Research by Other Groups

As of this report, we remain the only group that is, to our knowledge, actively pursuing irreversibility reduction strategies to achieve a significant improvement in engine efficiency. Most of the piston-engine research community remains engaged in SI- or CI-derived HCCI research as a means for efficiency improvement and emissions abatement. The most optimistic estimates cited are a 20% improvement in peak engine efficiency from HCCI. Based on our work, we believe that improvements closer to 10% might be actually realized. While this is an important gain in efficiency, we still consider the potential improvement of current incarnations of HCCI to be too small to meet GCEP targets.

A small group of researchers have considered, and based on our discussions with them, are currently reconsidering the potential of a low-irreversibility approach toward engine improvement. These include Profs. Dave Foster (University of Wisconsin-Madison) and Jerry Caton (Texas A&M University). Researchers at Sandia National Laboratory (Dr. Dennis Seibers) and Oak Ridge National Laboratory (Dr. Stuart Daw) are also considering activities in the area. During the past year, we met with both groups to explain the results of our work and to provide feedback as they consider complementary opportunities for the DOE engine program in this area.

Previous Results and Conclusions

In our previous work we have shown that while energy extraction during combustion can improve engine efficiency, this improvement comes about from a reduction of heat losses, not from a reduction of reaction irreversibility. To the contrary, the results indicated that for adiabatic systems, combustion irreversibility is minimized when the

reaction is allowed to proceed at constant (and minimum) volume. Understanding the ramifications of this observation in detail has been a key topic of research during this part year.

We have also shown that the general problem of efficient engine design can be approached from the perspective of exergy management. A key aspect of this work has been that the design space of simple-cycle engines is not nearly as broad as might have been thought and that a systematic approach to understanding engine architecture is therefore possible. While this was discussed in some detail for simple-cycle engines in last year's report, compound cycle engines were not considered and were left for future exploration.

Efforts in this Past Year

The report from last year focused mainly on the structuring of the engine architecture problem in terms of exergy management. Concurrent activities on piston engine optimization were not discussed at length because they were still of a preliminary nature. These activities were completed in the course of this year and therefore constitute the core of this report. While activities associated with the exergy/architecture problem have continued at a low level, there remain some details to be resolved before a comprehensive reporting of that work can be realized. As such, discussion of those activities is deferred to our final project report to be submitted this coming summer.

Results

Optimization of Nonadiabatic Engines

To determine the extent of piston engine efficiency improvement when the work extraction process is optimized, we solved an optimal control problem for a constrained dynamical system model of the engine, considering piston velocity profile as the only control input function. The model includes a single-step combustion mechanism as well as an empirical heat transfer term to account for the main source of energy dissipation from the system. The conventional slider-crank piston profile is used to initialize the gradient-based local optimization calculations. The analysis was described in brief in last year's report, Ref. 2. Details of the model and the numerical optimization algorithm are discussed in Pub. 1.

Figure 1 shows a set of control and state points which constitute a solution set for the optimal control problem. Compared to the slider-crank solution, the optimized piston motion yields increase in expansion work output of 2.6%. A feature unchanged from the slider-crank solution is that ignition still occurs close to the clearance volume V_{init}/CR at optimality (even though flexibility is built into the optimization algorithm to allow ignition away from the clearance volume). This maximizes system pressure, which maintains high expansion work output. On the other hand, the attendant high system temperature would also keep the heat loss rate high.
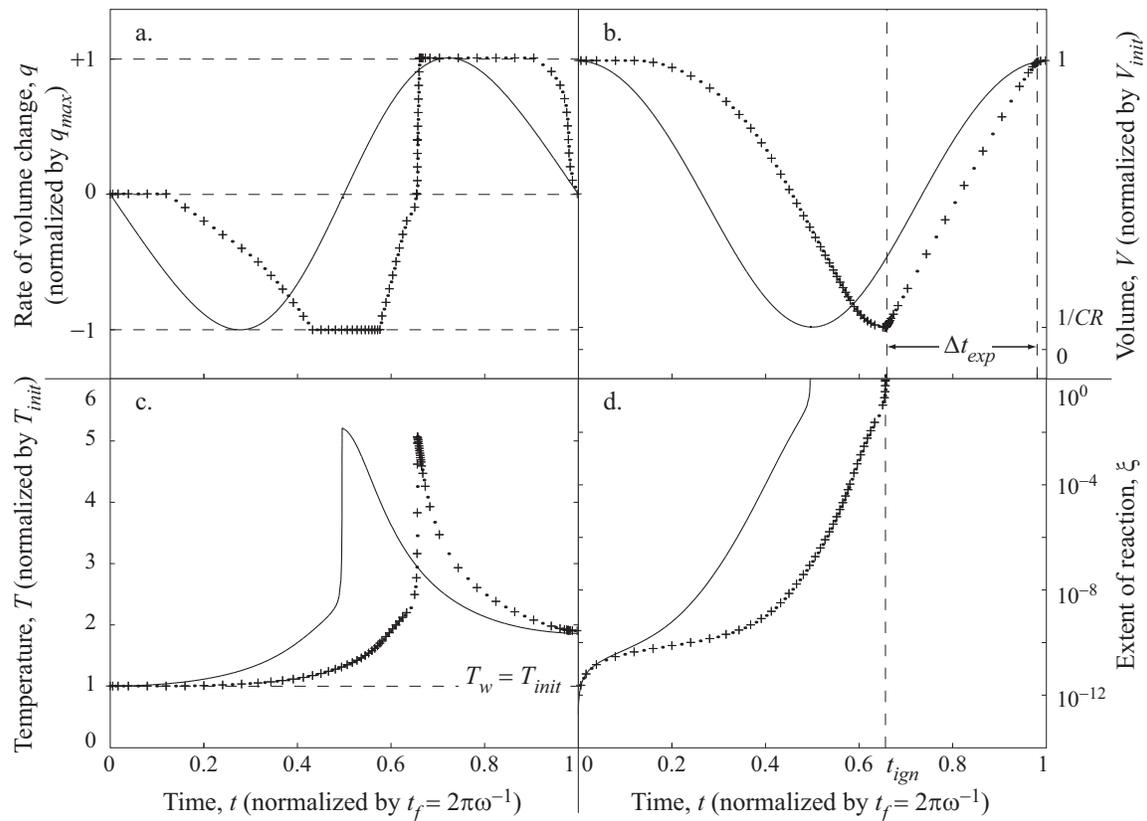
Figure 1: The optimal solution set (including control q, states V, T and ξ) as functions of time. The discrete control and state points are plotted at the grid points (shown as crosses) and at mid-intervals (shown as dots). For comparison, the slider-crank solution used to initialize the calculation is also shown as solid lines.

   Despite that, the engine efficiency improves as a consequence of lower *total* heat transfer loss, achieved by shortening the time spent at elevated temperatures. This is in turn accomplished by delaying the combustion phasing well beyond the process midpoint (TC of the slider-crank) and then expanding the product gases at the maximum allowable rate.

   Figure 1c also indicates that at optimality, the final temperature of the gas mixture is slightly higher as compared to the conventional case. Therefore, the efficiency increase cannot be attributed to reduction in exhaust (waste) enthalpy, but is due to lower heat transfer losses. This is reminiscent of results obtained in past studies of thermally insulated (low heat rejection) diesel engines (see, *e.g.*, Ref. 3). The explanation is straightforward: even though heat loss from the system is reduced, not all the available energy retained is extracted as work. Consequently, some amount is wasted in the form of exhaust gas at a higher temperature. Full utilization of the exergy that is retained would require the use of secondary expansion and/or heat recovery devices that are not considered in the present model.

The sensitivity of the optimal solution to three model parameters was also considered. Figure 2 shows similar optimal piston motion and extent of reaction profiles for the same engine operating at speeds ω = 1800 rpm and 2000 rpm: slow compression to the clearance volume at which point ignition occurs, followed by fast expansion to the initial volume. Figure 3 indicates that the optimal expansion work output increases with engine speed (solid line labeled "vary ω"). However, the slider-crank work output increases more over the same range of speeds. As a result, the efficiency gain via piston motion optimization diminishes from 2.6% to 1.6%.
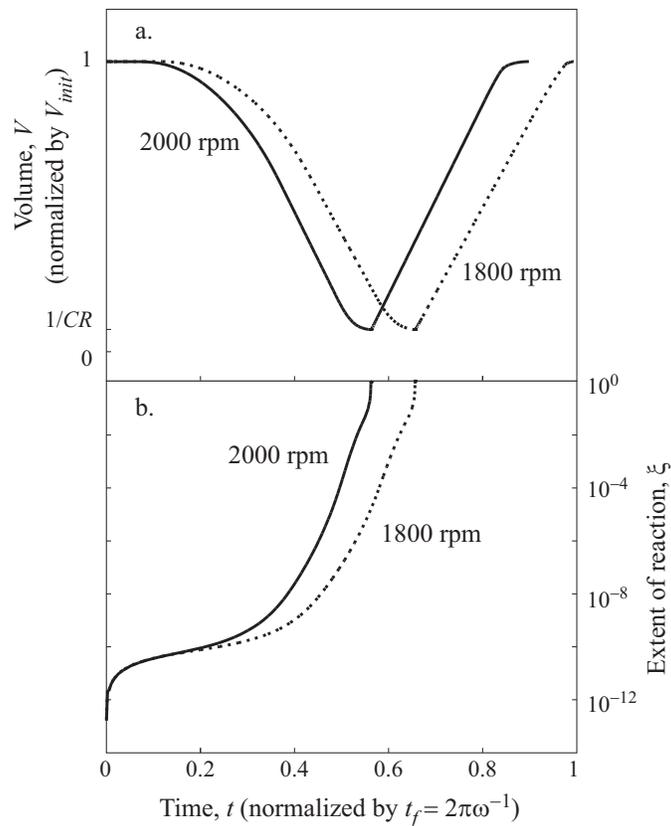

Figure 2: Comparison of the optimal solution sets for maximum expansion work output from a piston engine operating at two engine speeds, showing similar piston motion profiles of slow compression to the clearance volume—at which point the ignition occurs—followed by fast expansion to the initial volume.

For a given engine geometry, the maximum allowable rate of volume change (or, equivalently, the piston linear speed) varies directly with engine speed, $q_{max} \propto \omega$, whereas the cycle time varies inversely with speed, $t_f \propto \omega^{-1}$. Therefore, increasing the engine speed shortens the (total) cycle time t_f over which heat transfer occurs, as well as reducing the minimum time $\Delta V/q_{max}$ needed for the piston to displace some volume ΔV during expansion, when heat loss rate is high due to high post-combustion gas temperature.
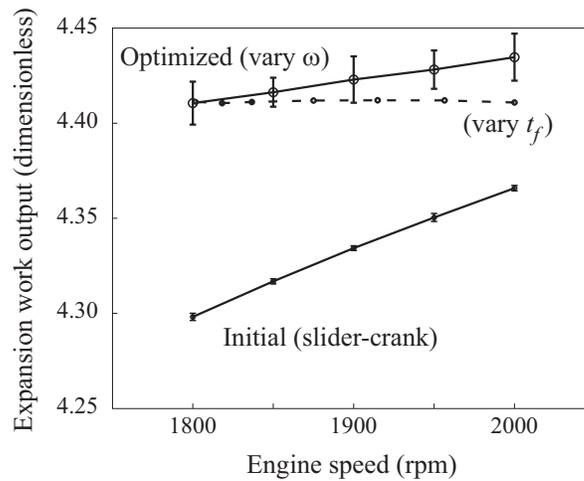
Figure 3: Variation of optimal expansion work output with engine rotational speed (solid line labeled "vary ω"), showing diminishing gain from slider-crank solution as speed increases. Optimal work output does not depend on the cycle time t_f if the maximum piston linear speed is fixed (dashed line labeled "vary t_f"). The average values and 95% confidence intervals shown are calculated based on 20 optimal solution sets.

A second set of calculations was used to de-convolve these two effects by studying the sensitivity of the optimal solution to cycle time while the maximum piston speed remains fixed. (As rotational speed ω increases and cycle time decreases, the maximum piston speed may be fixed by changing, to a certain extent, the slider-crank geometry, *i.e.* increasing the ratio of connecting rod to throw lengths.) Figure 3 shows that the optimal work output is approximately constant under these conditions (dashed line labeled "vary t_f").

Figure 4 shows how expansion work output varies with the mean wall temperature T_w used in the heat transfer model. Higher wall temperature reduces the temperature difference and therefore the rate of heat transfer loss from the hot post-combustion gas mixture to the cylinder wall. The optimized piston motion takes advantage of this effect, such that the overall expansion work output increases with the wall temperature.

In contrast, the initial (slider-crank) solutions show lower sensitivity to wall temperature changes. In fact, the expansion work output decreases slightly as wall temperature increases within the range considered in this set of calculations. The reason is that, within this range of wall temperatures, the slider-crank solutions yield over-advanced combustion phasing. Therefore, the reduction in heat transfer losses due to higher wall temperature further advances the phasing to *before* TC, which lowers the expansion work output. Within the range of wall temperatures considered, the efficiency gain via piston motion optimization varies from 2.3% to 2.9%.
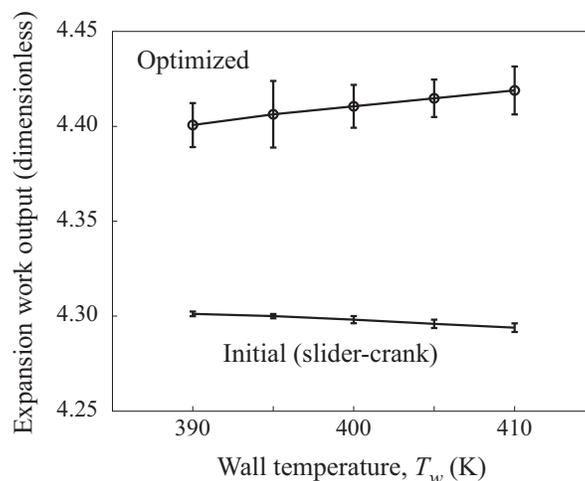
Figure 4: Variation of optimal expansion work output with mean wall temperature T_w. The average and 95% confidence intervals shown are calculated based on 20 optimal solution sets.

The results from these sensitivity studies, taken together, support the assertion that heat transfer at elevated temperatures is the dominant loss term being minimized in these optimization calculations. However, when compared to the conventional slider-crank piston profile, the increase in expansion work output via piston motion optimization never exceeds 3%. Considering the marginal potential for efficiency improvement—in particular when weighed against the engineering challenge of designing such an optimal engine—we decided not to continue the numerical piston motion optimization effort.

For the range of model parameters considered in the sensitivity studies, we also observed that the optimized combustion reaction always occurs close to the clearance volume (see, *e.g.*, Figure 1 and Figure 2). This suggests that unrestrained combustion reaction at the minimum allowable volume, while lossy in the exergetic sense, is likely to be as good as it gets. It is also reminiscent of the adiabatic system optimization results obtained previously (see 2004 annual report, Ref. 1): regardless of the dynamics involved, the optimal piston motion for an adiabatic reactive system is bang-bang (moving at either maximum compression or expansion speed) or, when constrained by the geometry, remains stationary (no work extraction, *i.e.*, reaction at constant volume). During this past year, we also revisited the adiabatic system analysis to arrive at a thermodynamic explanation for this optimal control strategy. The analysis and results are described in detail in Pubs. 2 and 3.

Optimization of Adiabatic Reactive Engines
<u>Optimal control problem description and solution</u>
The optimization problem, as presented previously in Ref. 1, seeks to maximize the expansion work output from a closed, adiabatic combustion piston engine. Recognizing that entropy-free boundary work is the only mode of energy transfer allowed for this system (whereas heat and mass transfers are absent, as are the associated entropy flows), the change in system entropy must equal the entropy generation due to chemical

reactions. In other words, the adiabatic ideal engine model isolates chemical reactions in the system as the sole source of entropy generation. We therefore recast the optimization problem to minimize the total entropy generation—which equals the overall change in system entropy over the time interval $[0, t_f]$—through optimal control of the piston motion.

To avoid quenching and incomplete reaction, we also require the gas mixture to react to near completion as defined by the entropy difference between its *instantaneous* thermodynamic state and the corresponding constant-*UV equilibrium* state, labeled $(\cdot)_{eq}$. This is the thermodynamic state which the system would have reached had it been isolated with internal energy U and volume V fixed at the instantaneous values, and with its *atomic* composition unchanged. By the second law, the total system entropy is maximized at this equilibrium condition, *i.e.*,

$$S_{eq}(U,V,\mathbf{N}_{eq}) \geq S(U,V,\mathbf{N}')$$

(1)

for all possible mixture compositions $\mathbf{N}'$ with the same atomic composition, including the actual composition $\mathbf{N}(t)$ of the system at the instant. We also note that Gibbs' equation reduces to

$$T_{eq}\mathrm{d}S_{eq} = \mathrm{d}U + P_{eq}\mathrm{d}V$$

(2)

by the definition of equilibrium state.

The revised optimal control problem, written in the standard form, is

$$\min \quad S_{gen} = S(U,V,\mathbf{N})\big|_{t=t_f} - S(U_0,V_0,\mathbf{N}_0)$$

$$\text{subject to} \quad \dot{U} = -P(U,V,\mathbf{N})\cdot q, \quad U(0)=U_0$$

$$\dot{N}_i = f_i(U,V,\mathbf{N}), \quad N_i(0)=N_{i,0}$$

$$\dot{V} = q, \quad V(0)=V_0$$

$$|q| \leq q_{max}$$

$$S_{eq}(U,V,\mathbf{N}_{eq})\big|_{t=t_f} \leq S(U,V,\mathbf{N})\big|_{t=t_f} + \varepsilon$$

$$V \geq V_{min}$$

(3)

In the absence of the minimum volume constraint $V \geq V_{min}$, it can be shown that the Hamiltonian of Problem (3) reduces to

$$H = -\alpha(\frac{P-P_{eq}}{T_{eq}})\cdot q - (1+\alpha)\frac{\mathrm{d}S}{\mathrm{d}t},$$

(4)

where the multiplier $\alpha \leq 0$. Therefore, the switching function is $-\alpha(P-P_{eq})/T_{eq}$, and by Pontryagin's maximum principle, the optimal bang-bang control that maximizes the Hamiltonian is

$$q^* = \begin{cases} -q_{max} & \text{if } P < P_{eq}, \\ +q_{max} & \text{if } P > P_{eq}. \end{cases} \tag{5}$$

Since the constant-UV reaction of common fuel/air mixtures is highly exothermic, the initial mixture pressure P_0 is lower than its corresponding equilibrium value $P_{eq,0}$. Therefore, the first stage of the optimal control strategy would be to compress the mixture at the maximum rate, until $P = P_{eq}$. The mixture is then expanded at the maximum rate as the system approaches complete reaction, $i.e.$, $S_{eq} - S \rightarrow 0$.

The analysis can be extended to solve Problem (3) with *active* minimum volume constraint $V \geq V_{min}$, yielding the optimal bang-bang control

$$q^* = \begin{cases} -q_{max} & \text{if } P < P_{eq} \text{ and } V > V_{min}, \\ 0 & \text{if } V = V_{min}, \\ +q_{max} & \text{if } P > P_{eq}. \end{cases} \tag{6}$$

The first three stages of the optimal control that minimizes the entropy generated in an adiabatic reactive piston engine subject to the minimum volume constraint are therefore (a) rapid compression of the reactant mixture to the minimum allowable volume; (b) maintaining the mixture at the minimum volume until the system pressure equals its constant-UV equilibrium value; followed by (c) rapid expansion as the system approaches complete reaction.

Equilibrium entropy minimization as the optimal strategy
Absent the minimum volume constraint, it can be shown that the entropy difference $L = S_{eq} - S$ is a Lyapunov function. This means that the constant-UV equilibrium thermodynamic states are stable (in the Lyapunov sense) and that the equilibrium states serve as attractors for the system at any point on the state space $(U, V, \mathbf{N})$. In this case, the equilibrium Gibbs' relation, Eq. (2), combined with the first law, $dU = -PdV$, reduces the Hamiltonian to

$$H = \alpha \frac{dS_{eq}}{dt} - (1+\alpha) \frac{dS}{dt} = \alpha \frac{dL}{dt} - \frac{dS}{dt}. \tag{7}$$

At any time t, one has no control over the instantaneous rate of entropy change dS/dt for the adiabatic system, which is set by the chemical kinetics and the state at that time. Instead, the maximum principle calls for choosing the control input that minimizes dL/dt, which is a function of the rate of volume change q (the control input) as well as the state $(U, V, \mathbf{N})$. This, in turn, means that the optimal control minimizes the equilibrium entropy S_{eq}, to which the system is attracted.

In retrospect, the reason that equilibrium entropy minimization is optimal is straightforward. The objective in Problem (3) to be minimized is the final entropy $S(t_f)$, required to be some distance ε away from its constant-UV equilibrium. Since ε is defined

a priori, it follows that the optimal control strategy calls for minimizing the corresponding equilibrium entropy S_{eq}.

For an adiabatic system, the relationship $dU_{eq} = dU = -PdV = -PdV_{eq}$ holds when the subscript $(\cdot)_{eq}$ refers to the constant-UV equilibrium. This means that Gibbs' equation at equilibrium, Eq. (2), can be written as

$$T_{eq}dS_{eq} = (1 - \frac{P_{eq}}{P})dU. \tag{8}$$

The optimal strategy of equilibrium entropy minimization therefore translates to either compression (and $dU > 0$) of the reacting gases if the pressure ratio P_{eq}/P is greater than unity, or expansion ($dU < 0$) if $P_{eq}/P < 1$.

Numerical examples

A series of three numerical examples are used to illustrate the results discussed above. Some of the model parameters used in the nonadiabatic numerical optimization study are retained, $e.g.$, the engine geometry, compression ratio $CR = 13$, engine speed $\omega_0 = 1800$ rpm, and thus the maximum allowable rate of volume change q_{max}. The initial temperature T_0 was chosen such that ignition occurs very close to the clearance volume $V_{min} = V_0/CR$ (top-center) of the slider-crank engine. The reaction completion parameter ε was fixed at $10^{-4}L_0$, where $L_0 = S_{eq}(U_0, V_0, \mathbf{N}_{eq,0}) - S(U_0, V_0, \mathbf{N}_0) = 1.3$ kJ/kg$_{mix}$-K is the difference in entropy between the initial state and its corresponding equilibrium. The GRI-Mech 3.0 natural gas combustion mechanism is used in the simulations.

Figure 5 compares the feasible—but non-optimal—slider-crank solution (in red) to the optimal solutions for Problem (3) with the minimum volume constraint (in blue, labeled $(\cdot)_v^*$) and without (in black, labeled $(\cdot)^*$). The plots on the second and the fourth columns highlight the optimal control inputs and the state responses near the bang-bang control switches, marked **S** (for **S**witching), or in the volume-constrained case, **N** and **X** (for e**N**tering and e**X**iting the constraint) on the volume profiles (row 2 on Figure 5).

The optimal solutions shown are computed based on the analytical results, Eqs. (5) and (6), which are not $explicitly$ dependent on the choice of the reaction mechanism. However, the detailed kinetics affects the instantaneous mixture composition, temperature, and thus pressure, which in turn determines the optimal switching time. For instance, in the case without the volume constraint, the reactant mixture is compressed beyond the volume ratio of $CR = 13$ before ignition (indicated by the precipitous decrease in fuel (propane) mole number N_{fuel}), leading to pressure P—as determined by the reaction mechanism—equaling the corresponding equilibrium pressure P_{eq}, at which point the product gases are expanded.

The function $L = S_{eq} - S$ being Lyapunov also means that the optimal extent "deficit" plots (row 5, columns 1 through 4 on Figure 5) can be interpreted as showing the optimal final times $t_{f,v}^*(\xi_f)$ and $t_f^*(\xi_f)$ (on the horizontal axes) as monotonically increasing functions of the parameter ξ_f (on the vertical axes) for the terminal inequality constraint $L(t_f) = S_{eq}(t_f) - S(t_f) \leq (1 - \xi_f) L_0$.
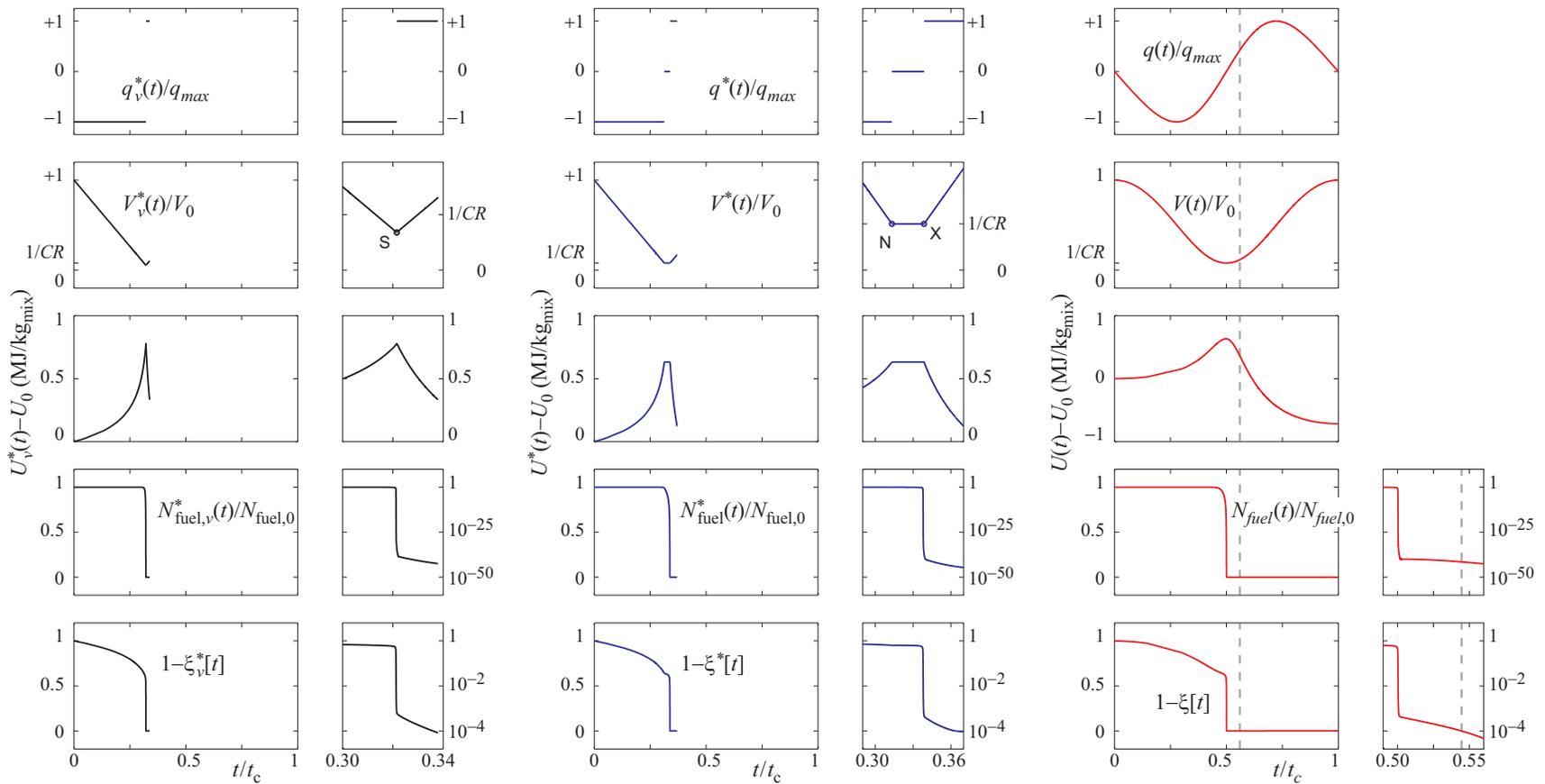
Figure 5: Comparison of control input q, states V, U, N_{fuel}, and the entropy-based extent of reaction "deficit" $1-\xi = L/L_0$ as functions of time t (normalized by the period $t_c = 1/30$ sec).

- Left (Columns 1 and 2 / black / labeled $(\cdot)_v^*$): the optimal solution for Problem (3) without the minimum volume constraint;
- Center (Columns 3, 4 / blue / labeled $(\cdot)^*$): the optimal solution for Problem (3) with the minimum volume constraint; and
- Right (Columns 5, 6 / red / -): the slider-crank solution, which is feasible but non-optimal.

Figure 6 compares the entropy generation from the optimal systems to that from the non-optimal, slider-crank system. Given an extent parameter ξ (or correspondingly, a reaction completion parameter $\varepsilon = (1 - \xi_f) L_0$), the figure shows that $S_{gen,sc} \geq S_{gen}^* \geq S_{gen,v}^*$ when all three systems react to that same extent.
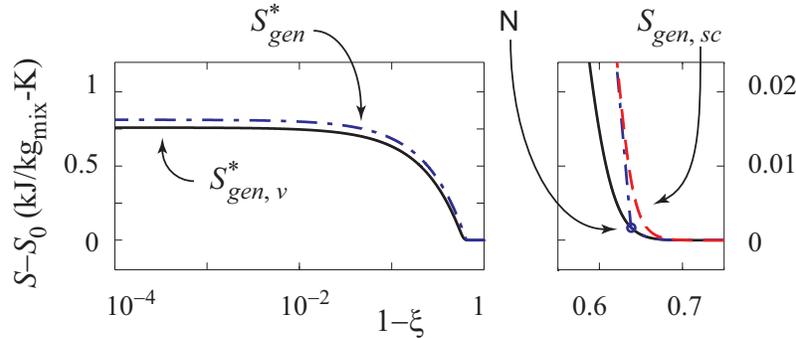

Figure 6: Comparison of the entropy generated by the optimal systems versus that by the non-optimal slider-crank system, plotted as functions of the extent "deficit" $1-\xi = L/L_0$. The $S_{gen,sc}$ line is not shown on the left plot because it is not distinguishable from the S_{gen}^* line at the given vertical scale. For the volume-constrained system, the constraint becomes active at the point labeled **N**.

The first inequality $S_{gen,sc} \geq S_{gen}^*$ is simply the definition of an optimal solution. The slider-crank line $S_{gen,sc}$ (red, dashed) begins to deviate noticeably from the optimal S_{gen}^* line (blue, dash-dotted) at $\xi > 0.3$, as highlighted on the right. This is because it takes the slider-crank system longer to complete the compression stroke, allowing relatively more time for partial oxidation (and entropy generation) of the fuel/air mixture prior to ignition. However, subsequent difference between the two quantities is miniscule, since ignition—which accounts for most of the entropy generated—occurs at essentially the same minimum (clearance) volume for both systems. At extent of reaction $\xi = 0.9999$ ($\varepsilon = 10^{-4}L_0$), the "excess" entropy generated from the slider-crank system as compared to the optimal system is less than 0.1 J/kg$_{mix}$-K and is not distinguishable on the vertical scale used on the left.

The second inequality $S_{gen}^* \geq S_{gen,v}^*$ arises because the set of admissible control inputs—*i.e.*, the set of acceptable piston motion profiles $\{q(t)\}$ —for Problem (3) *including* the minimum volume constraint is a subset of control inputs $\{q_v(t)\}$ for the variant problem *excluding* the constraint. In other words, there is a "richer" set of control inputs which solve the variant unconstrained problem. Therefore, the corresponding (minimum) objective functions are related by

$$S_{gen}^* = \min_{\{q(t)\}} S_{gen} \geq \min_{\{q_v(t)\}} S_{gen} = S_{gen,v}^* \tag{9}$$

The right plot of Figure 6 shows that the two optimal entropy generation lines overlap until the minimum volume constraint becomes active (labeled **N**), at which point they deviate. Most of the "excess" entropy generated from the volume-constrained optimal system compared to the unconstrained one, $S_{gen}^* - S_{gen,v}^*$ is due to the ignition occurring at

a larger volume for the former ($=V_{min}$) as compared to the latter ($<V_{min}$). At extent of reaction $\xi = 0.9999$, the difference is about 50 J/kg$_{mix}$-K.

The general conclusion of this analysis—that equilibrium entropy minimization is the optimal strategy—is best depicted on internal energy/entropy (U, S) diagrams as shown on Figure 7. The figure shows the optimal U, S trajectories as well as the corresponding U, S_{eq} equilibrium trajectories for both the volume-constrained and unconstrained systems. The latter trajectories, shown as dash-dotted lines, indicate that the reacting gas mixture is indeed being manipulated such that the equilibrium entropy is constantly decreasing, both at the initial reactant stage when the system pressure is far below its corresponding equilibrium pressure (upper plot of Figure 7) as well as after ignition when the system pressure overshoots its equilibrium value and the reaction approaches completion (highlighted on the lower plots of Figure 7).
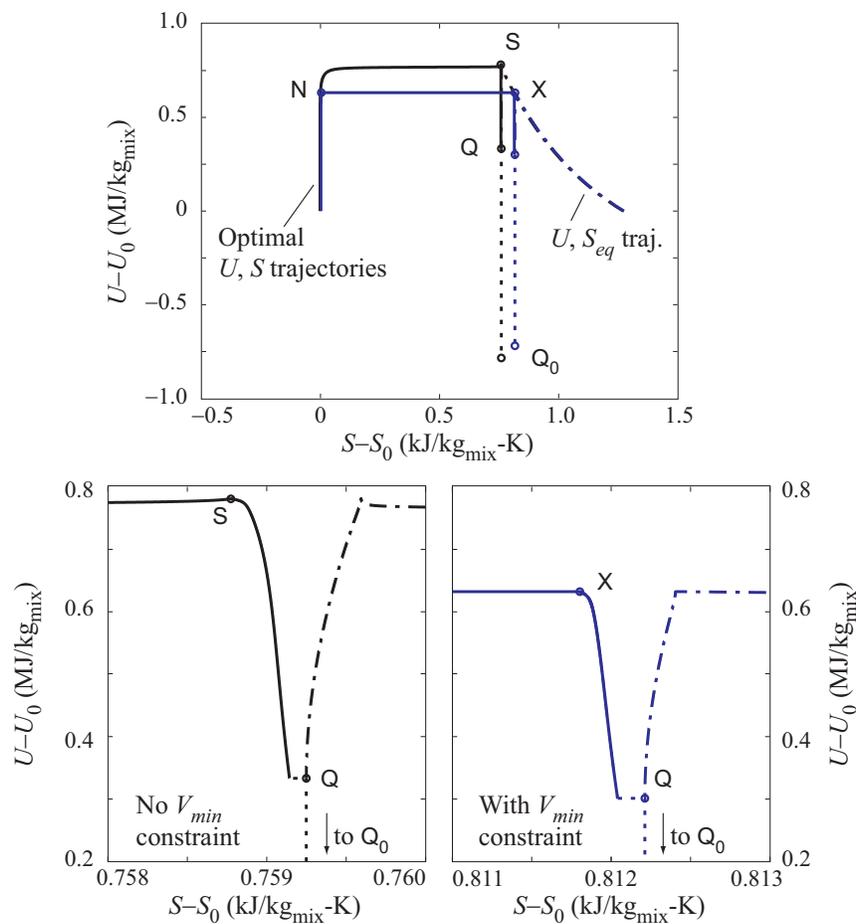

Figure 7: The internal energy/entropy (U, S) diagrams for adiabatic systems given optimally controlled piston motion profiles. The actual trajectories (solid) and the corresponding constant-UV equilibrium trajectories (dash-dotted) are shown for systems with active minimum volume constraint (blue) and without (black). Suboptimal trajectories when the symmetric expansion constraint is added are also shown (dotted lines).

<u>A suboptimal solution for expansion work maximization</u>
    We note that a terminal constraint, either in the volume form

$$V(t_f) \geq V_f, \tag{10}$$

or in terms of pressure,

$$P(t_f) \leq P_f, \tag{11}$$

needs to be appended to Problem (3) to ensure full expansion of the high pressure
combustion product gases to either some final volume V_f (*e.g.*, symmetric expansion to
the initial volume, $V_f = V_0$) or final pressure P_f (*e.g.*, optimal expansion to the
atmospheric pressure, $P_f = 1$ atm). However, we are thus far unable to solve the extended
optimal control problem because adding either Constraint (10) or (11) would invalidate
the control synthesis reported here. In particular, we are unable to argue with
mathematical rigor that the function $L = S_{eq} - S$ is Lyapunov when either constraint is
introduced.

    Nevertheless, an adequate suboptimal solution for the optimal control problem with
full expansion can be devised based on the results obtained thus far. The control would
follow the optimal strategy per Equation (5) or (6), and then react at constant volume to
reach the minimum equilibrium entropy state (labeled **Q**—for e**Q**uilibrium—on Figure
7). The equilibrated mixture can then be expanded quasistatically to some final state V_f
or P_f.

    Figure 7 illustrates the state trajectories using this suboptimal control for a symmetric
expansion constraint $V_f = V_0$, shown as dotted lines horizontally across and vertically
down to the final states labeled **Q**$_0$. More important than the detailed trajectories is the
recognition that the final entropy of the optimal *and* fully-expanded system is bounded
above by the value S_{eq} at equilibrium state **Q**. In other words, the entropy generation for
the full-expansion optimal system will not exceed that for the original optimal system
(considered in Problem (3)) by more than the quantity ε, which is very small for common
fuel/air systems, as the numerical examples above exemplify.

Concluding Remarks/Future Plans
    Both the nonadiabatic piston engine optimization results and the insight gained from
revisiting the adiabatic system optimization problem reiterate the value of approaching
the engine design problem from the exergy viewpoint.
    In the nonadiabatic case, the numerical optimization takes into consideration the
interplay between various terms in the exergy balance equation. The solutions suggest
that the additional entropy generation (exergy destruction) incurred by combusting at a
larger mixture volume as well as the subsequent incomplete expansion (high exergy
exhaust, low exergy transfer in the form of work) would offset any reduction in exergy
loss via heat transfer as a result of lower post-combustion temperature. The resulting
increase in expansion work output was found to be less than 3%. While the model used
in these calculations may be further refined, we expect the efficiency improvement to

remain modest compared to the theoretical (exergetic) limits due to significant heat transfer losses.

In the ideal, adiabatic case, we are able to relate the extremal (bang-bang) piston motion obtained via Pontryagin's maximum principle to the simple thermodynamic principle of entropy generation minimization (*i.e.*, exergy destruction minimization). We are initiating a research effort to establish the viability of such a strategy in the laboratory using an ultra-fast compression-expansion machine. If successful, this work will pave the way for the design of ultra-efficient engines.

Publications
1. Teh, K.-Y., C.F. Edwards, "Piston Motion Optimization to Maximize Work Output from an Internal Combustion Engine," submitted to the ASME International Mechanical Engineering Congress & Exposition, Chicago, IL 2006.
2. Teh, K.-Y., C.F. Edwards, "An Optimal Control Approach to Minimizing Entropy Generation in an Adiabatic Internal Combustion Engine," submitted to the 45th IEEE Conference on Decision and Control, San Diego, CA 2006.
3. Teh, K.-Y., C.F. Edwards, "An Optimal Control Approach to Minimizing Entropy Generation in an Adiabatic IC Engine with Fixed Compression Ratio," submitted to the ASME International Mechanical Engineering Congress & Exposition, Chicago, IL 2006.

References
1. Edwards, C.F., K.-Y. Teh, S.L. Miller, P.A. Caton, "Development of Low-Irreversibility Engines," GCEP Annual Report, 2004.
2. Edwards, C.F., K.-Y. Teh, S.L. Miller, P.A. Caton, H. Song, "Development of Low-Irreversibility Engines," GCEP Annual Report, 2005.
3. Primus, R.J., K.L. Hoag, P.F. Flynn, M.C. Brands, "An Appraisal of Advanced Engine Concepts Using Second Law Analysis Techniques," SAE Paper 841287, 1984.

Contact
C.F. Edwards: cfe@stanford.edu